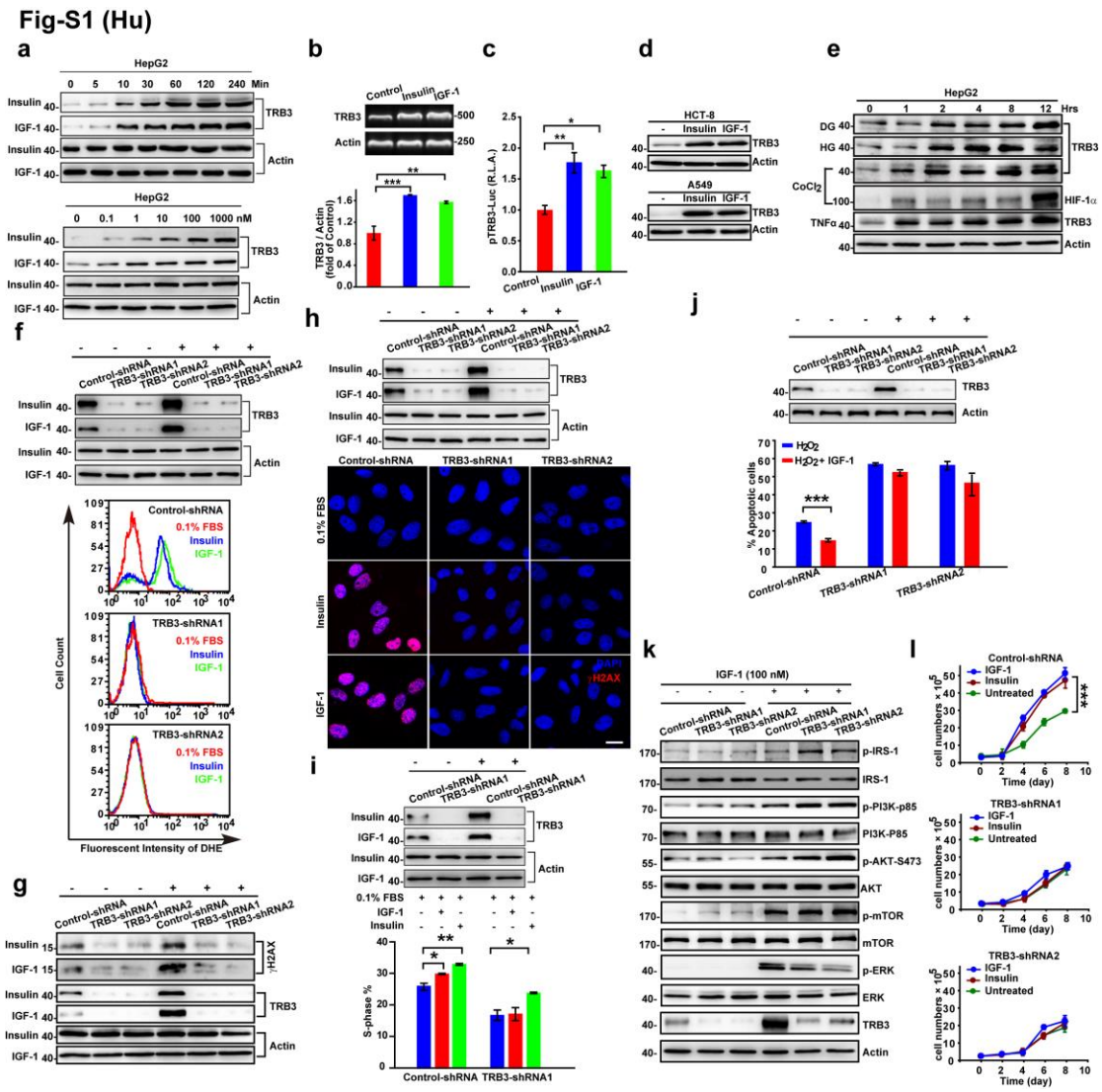

Supplementary Figure 1. Metabolic stress induced TRB3 mediates the cancer-promoting roles. (**a**) HepG2 cells were treated with insulin/IGF-1 (100 nM) for indicated times (upper) or treated with insulin/IGF-1 at different concentrations for 12 hours. The expression of TRB3 was detected with immunoblotting. Data are representative immunoblots of 5 independent assays. (**b**) HepG2 cells were treated with insulin (100 nM) or IGF-1 (100 nM) for 12 hours. RT-PCR analysis was carried out to determine the mRNA level of TRB3 and β-actin. Data are mean ± s.e.m. of 3 independent assays with triplicates. (**c**) HepG2 cells were transfected with pTRB3-luc plasmid for 24

hours. The cells were treated with insulin (100 nM) or IGF-1 (100 nM) for another 12 hours and the luciferase activity was measured. Data are mean ± s.e.m. of 5 independent assays with triplicates. (**d**) HCT-8 or A549 cells were treated with insulin (100 nM)/IGF-1 (100 nM) for 4 hours. The TRB3 levels were determined with immunoblot (*n*=5 independent assays). (**e**) HepG2 cells were treated with glucose deprivation (DG), high glucose (HG, 50 mM), $CoCl_2$ (200 μM) and TNFα (50 ng ml^{-1}) for indicated time points respectively. TRB3 levels were determined with immunoblot analysis (*n*=5 independent assays). (**f**) TRB3 depletion suppressed insulin/IGF-1-induced ROS generation. ROS was determined with Dihydroethidium (DHE, 10 μM) staining followed with flow cytometry (*n*=5 independent assays). (**g**,**h**) TRB3 depletion attenuated insulin/IGF-1-induced DNA damage. The expression of γH2AX was evaluated with immunoblotting (g) or immuno-fluorescence staining (h), scale bar, 18.75 μm, *n*=5 independent assays. (**i**) TRB3 depletion decreased the S-phase fraction and inhibited the insulin/IGF-induced prolongation of S-phase. Data are mean ± s.e.m. of 3 independent assays with triplicates. (**j**) TRB3 depletion increased sensitivity of cancer cells to hydrogen peroxide-induced apoptosis. Data are mean ± s.e.m. of 3 independent assays with triplicates. (**k**) HepG2 cells were treated with or without IGF-1 for 30 min and expressions of indicated proteins were detected with immunoblotting (*n*=5 independent assays). (**l**) Depletion of TRB3 inhibited insulin/IGF-1-induced proliferation of cancer cells. Data are mean ± s.e.m. of 3 independent assays with triplicates.

Statistical significance was determined by Student's *t*-test; **P*<0.05; ***P*<0.01; ****P*<0.001.

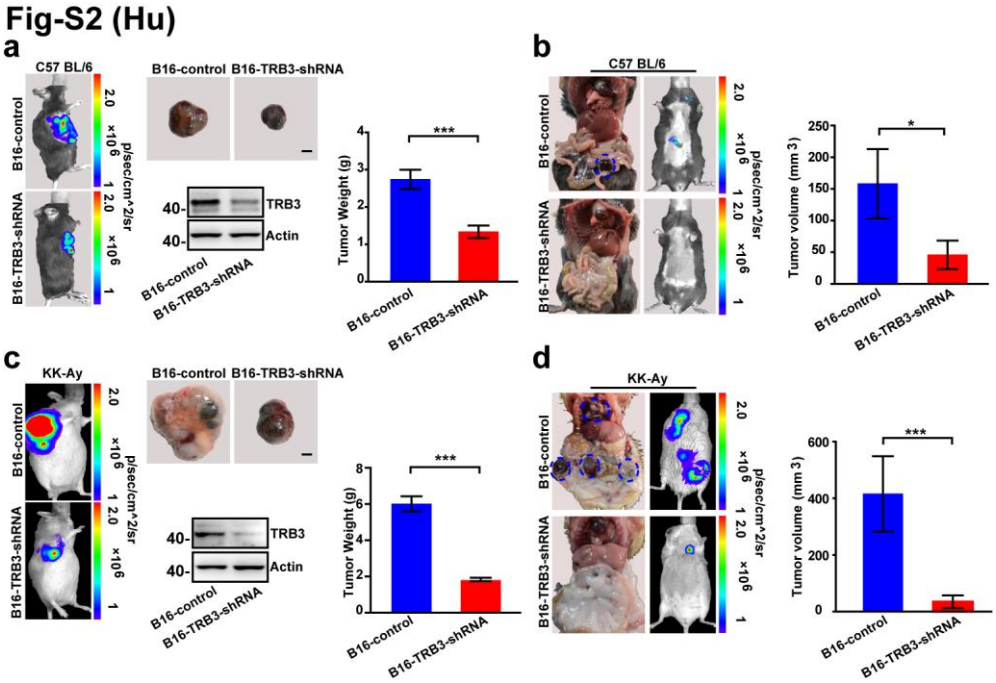

Supplementary Figure 2.TRB3 depletionin tumor cells displays much prominent antitumour effects in diabetic KK-Ay mice than that in C57BL/6 mice. (**a**) C57 BL/6 mice were *s.c.* inoculated with B16-F10 cells expressing control-shRNA or TRB3-shRNA (1.5×10^5). Data are representative bioluminescence images and tumours along with quantified tumour weight. The levels of TRB3 were also shown in B16-F10 cells expressing control-shRNA or TRB3-shRNA. Scale bar, 1.5 cm, *n*=8 per group. (**b**) C57 BL/6 mice were *i.v.* injected with B16-F10 cells expressing control-shRNA or TRB3-shRNA (3×10^5). Data are bioluminescence images with total tumour volumes at multiple metastatic sites (mean ± s.e.m.; *n*=8 per group). (**c**) KK-Ay T2D mice were *s.c.* inoculated with B16-F10 cells expressing control-shRNA or

TRB3-shRNA (1.5×10^5). Data are representative bioluminescence images and tumours along with quantified tumour weight. The levels of TRB3 were also shown in B16-F10 cells expressing control-shRNA or TRB3-shRNA. Scale bar, 1.5 cm, n=8 per group. (**d**) KK-Ay T2D mice were *i.v.* injected with B16-F10 cells expressing control-shRNA or TRB3-shRNA (3×10^5). Data are bioluminescence images with total tumour volumes at multiple metastatic sites (mean ± s.e.m.; n=8 per group). Statistical significance was determined with Student's *t*-test; *P<0.05, ***P<0.001.

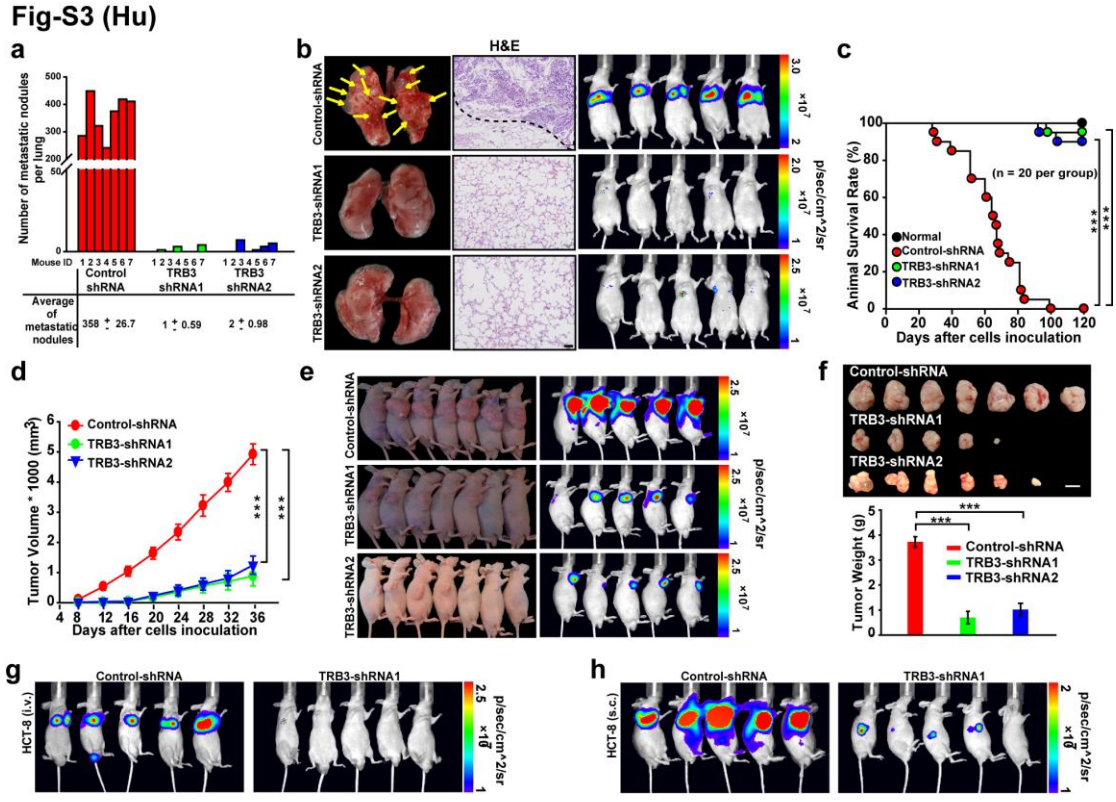

Supplementary Figure 3. TRB3 depletion protects against tumour metastasis and growth. (**a,b**) BALB/c nude mice were *i.v.* injected with HepG2 cells expressing control-shRNA, TRB3-shRNA1 or TRB3-shRNA2

(3×10^6). *In vivo* imaging system was used to detect tumour metastasis. Data are number of metastases in lungs (a). Representative graphs of lungs, H&E stained lung sections and bioluminescence imaging (b). Metastatic nodules were indicated by arrows. Scale bar, 5 μm, n=10 per group. (**c**) Kaplan-Meier survival curve for mice harboring tumours expressing control-shRNA or one of the two shRNAs targeting TRB3 (n=20 per group). Statistical significance was determined by Kaplan-Meier log-rank test; ***P<0.001. (**d**) HepG2 cells expressing control-shRNA, TRB3-shRNA1 or TRB3-shRNA2 (1.5×10^6) were *s.c.* injected into the right flank of the BALB/c nude mice. Data are mean volumes ± s.e.m. at indicated times and photographs of representative mice (n=10 per group). (**e,f**) Data are photographs of representative mice (e), and tumours along with quantified tumour weight (f). Scale bar, 1.5 cm, n=10 per group. (**g,h**) BALB/c nude mice were *i.v.* (3×10^6) or *s.c.* (1.5×10^6) injected with HCT-8 cells expressing control-shRNA or TRB3-shRNA1. *In vivo* imaging system was used to detect tumour metastasis and growth. Data are representative bio-photonic images of animals with metastasis (g) and growth (h) (n=6 per group). Statistical significance was determined by Student's t-test; ***P<0.001.

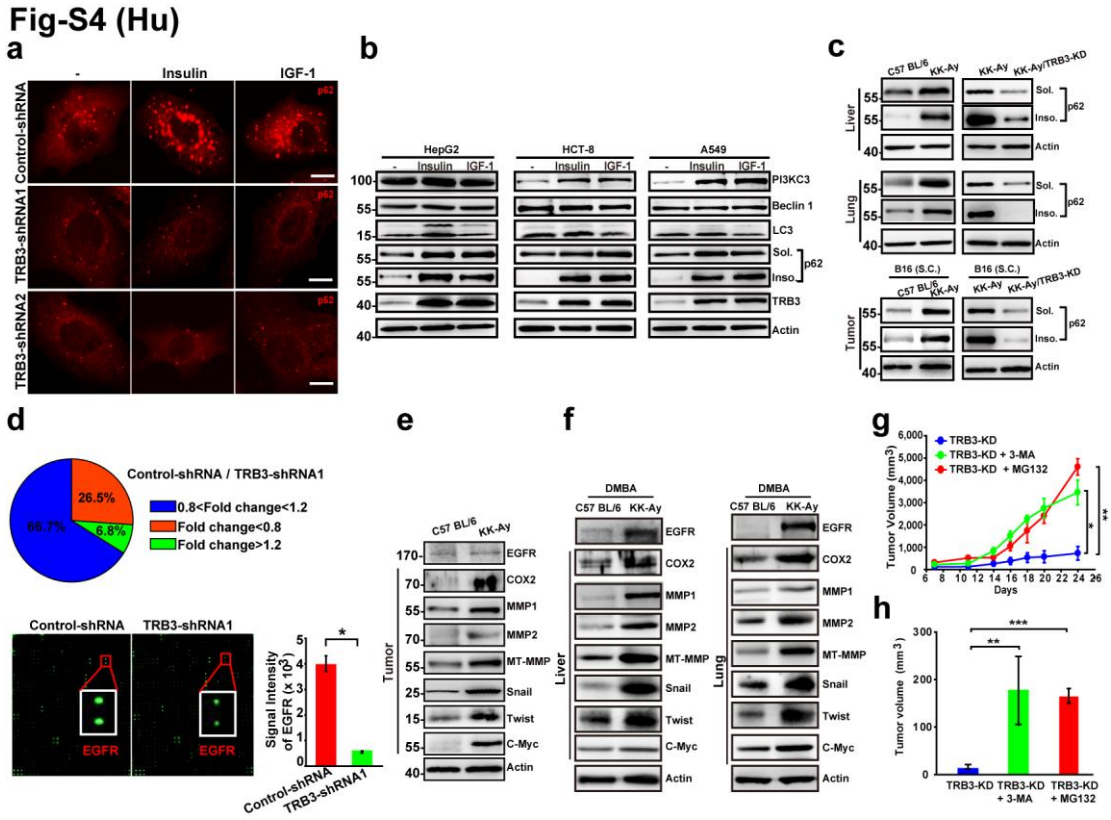

Supplementary Figure 4. Metabolic stresses induce autophagy inhibition and tumour-promoting factor accumulation. (**a**) HepG2 cells were treated with the indicated stimulators for 12 hr and p62 expression was evaluated with an indirect immunofluorescence (*n*=3 independent assays). Scale bar, 7.5 μm. (**b**) HepG2, HCT-8 and A549 cells were treated with or without insulin/IGF-1 (100 nM) for 12 hours. The expressions of autophagy related proteins were evaluated with immunoblotting (*n*=5 independent assays). (**c**) The expression of soluble and insoluble p62 in liver, lung tissues and xenograf ttumours were evaluated with immune-blotting in C57 BL/6, KK-Ay and KK-Ay/TRB3-KD mice. Data are representative immunoblots of 4 independent assays. (**d**) The cell-wide protein expression was evaluated with Human L-1000 Antibody Arrays in HepG2 cells expressing TRB3-shRNA1 or

control-shRNA. Data are the summarized fold changes of proteins (control-shRNA/TRB3-shRNA1) (upper) and representative spots showing differentially expressed EGFR (framed) (lower). Data are representative of 2 independent assays. (**e**) The xenograft tumours express higher pro-metastasis and pro-EMT factors in KK-Ay mice than that in C57 BL/6 mice. Data are representative immunoblots of 4 independent assays. (**f**) The liver and lung tissues express higher pro-metastasis and pro-EMT factors in DMBA-treated KK-Ay mice than that in DMBA-treated C57 BL/6. Data are representative immunoblots of 4 independent assays. (**g,h**) Suppressing autophagy or UPS reverses the antitumour effect of TRB3 knockdown. TRB3 knockdown KK-Ay mice were *s.c.* injected with B16-F10 cells (1.5×10^5) or *i.v.* injected with B16-F10 cells (3×10^5) after infection. The mice were treated with 3-MA (30 mg kg^{-1} per day) or MG132 (2.5 mg kg^{-1}, twice a week) from day 7 after tumour inoculation. Data are mean ± s.e.m. of tumour growth curve (g) and total tumour volumes in multiple metastatic sites (h) (n=6 per group). Statistical significance was determined by Student's t-test; *P<0.05, **P<0.01, ***P<0.001.

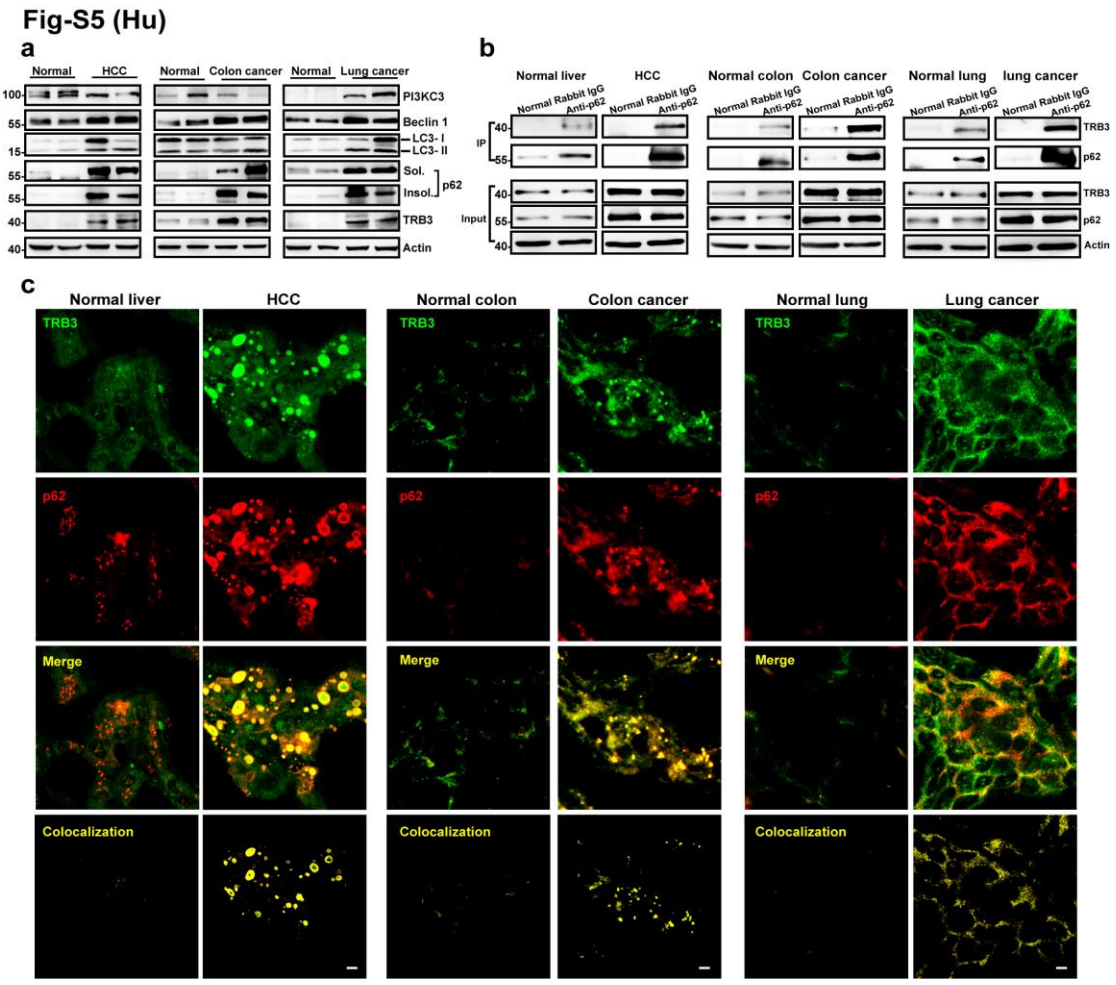

Supplementary Figure 5. The interaction of TRB3/p62 is enhanced in human tumourtissues. (**a**) Expressions of autophagy molecules in HCC, colon and lung cancer tissues were evaluated with immunoblotting (*n*=5 cases). Normal tissue extracts were used as control (*n*=3 cases). Data are representative immunoblots of 3 independent assays. (**b**) Co-IP of endogenous TRB3 and p62 proteins from fresh normal human (*n*=3 cases) and tumour tissue (*n*=5 cases) samples. Tissue extracts were IP with anti-p62 Ab or rabbit IgG and blotted with anti-TRB3 Ab. (**c**) Human normal and cancer tissue array slides were double immunostained with anti-TRB3 (green) or anti-p62 (red) Ab. Double staining in yellow shows TRB3/p62co-localization. Scale

bar, 5 μm. Each columnis representative of double-stain (*n*=10 cases).

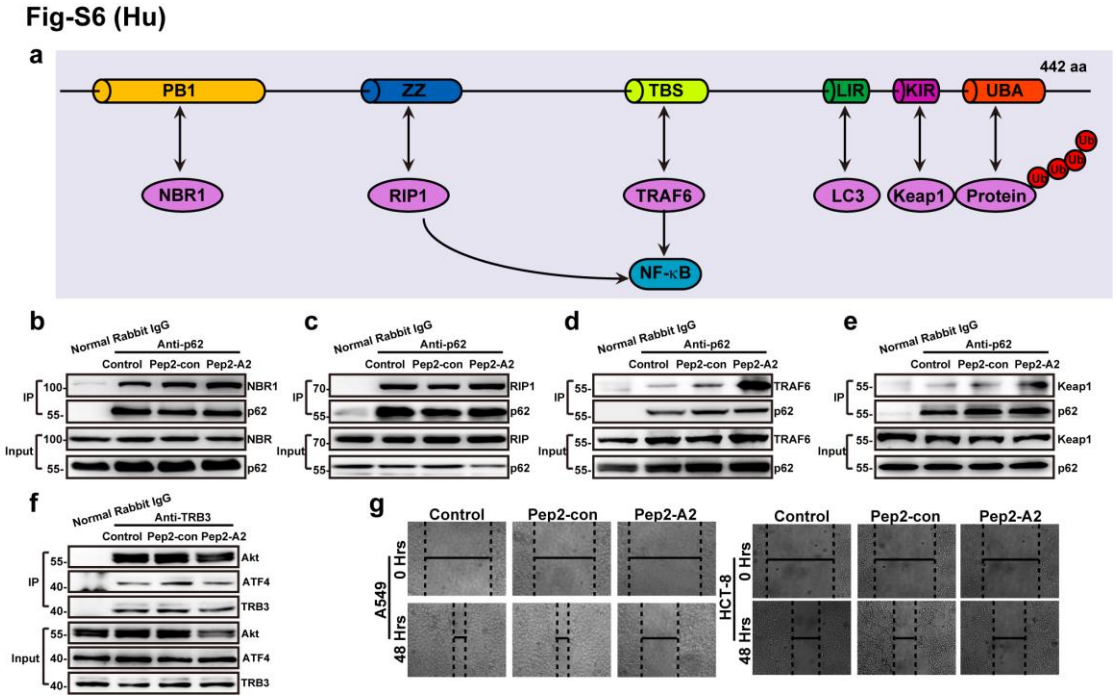

Supplementary Figure 6. Pep2-A2 treatment increases the binding of p62 to TRAF6 and Keap1. (**a**) Domain structure of p62. (**b-e**) The extracts of HepG2 cells treated with Pep2-con or Pep2-A2 were IP with an anti-p62 Ab or normal rabbit IgG and blotted with anti-NBR1, anti-RIP1, anti-TRAF6 or anti-Keap1 Ab. Data are representative immunoblots of 3 independent assays. (**f**) The extracts of HepG2 cells treated with Pep2-con or Pep2-A2 were IP with an anti-TRB3 Ab or normal rabbit IgG and blotted with anti-AKT or anti-ATF4 Ab. Data are representative immunoblots of 3 independent assays. (**g**) Wound healing assay was conducted in A549 and HCT-8 cells treated with 5 μM of Pep2-A2 or Pep2-con at the indicated times. Data are representative of 3 independent assays.

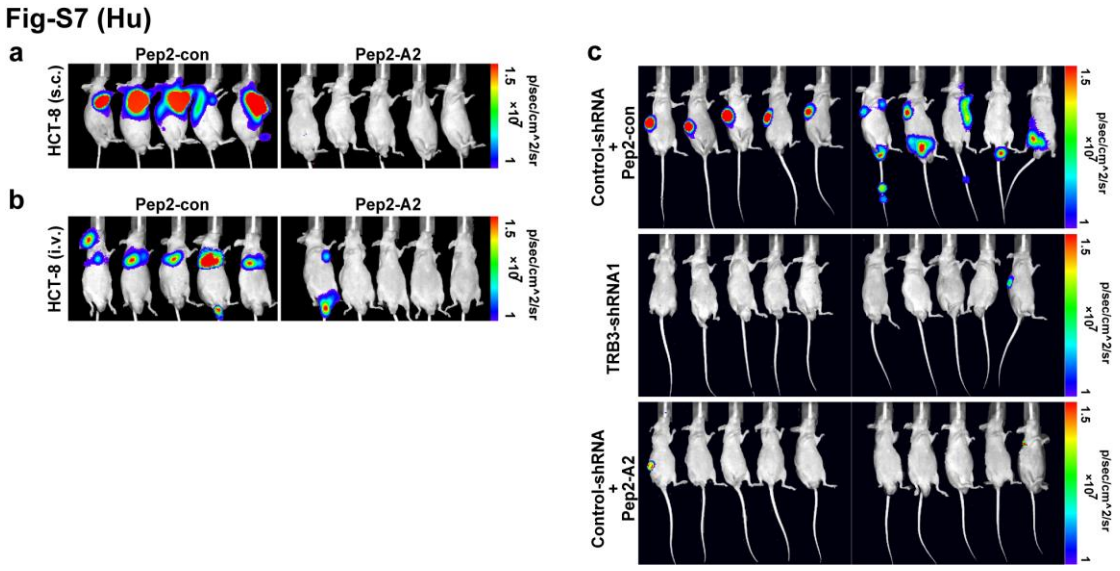

Supplementary Figure 7. The Pep2-A2 treatment inhibits tumour development and progression. (**a**, **b**) Nude mice were *s.c.* or *i.v.* inoculated with HCT-8 cells into the right flank ($1.5x10^6$) or the lateral tail vein ($3x10^6$). One week after tumour inoculation, mice were *i.v.* treated with the Pep2-A2 or Pep2-con (5 mg kg^{-1}) twice a week for 5 weeks. Data are representative bio-photonic images (*n*=6 per group). (**c**) Pep2-A2 inhibits primary recurrence and multi-organ metastasis. Nude mice were *s.c.* inoculated with HepG2 cells expressing control-shRNA1 (*n*=20) or TRB3-shRNA2 (*n*=10). When tumours reached a volume of 300 mm^3, tumour resection was performed. The control-shRNA mice (n=10) were randomly selected for treating with Pep2-A2 for 2 months (5 mg kg^{-1}, *i.v.*, beginning 1 day post-resection). Data are representative bio-photonic images of animals with primary tumour recurrence.

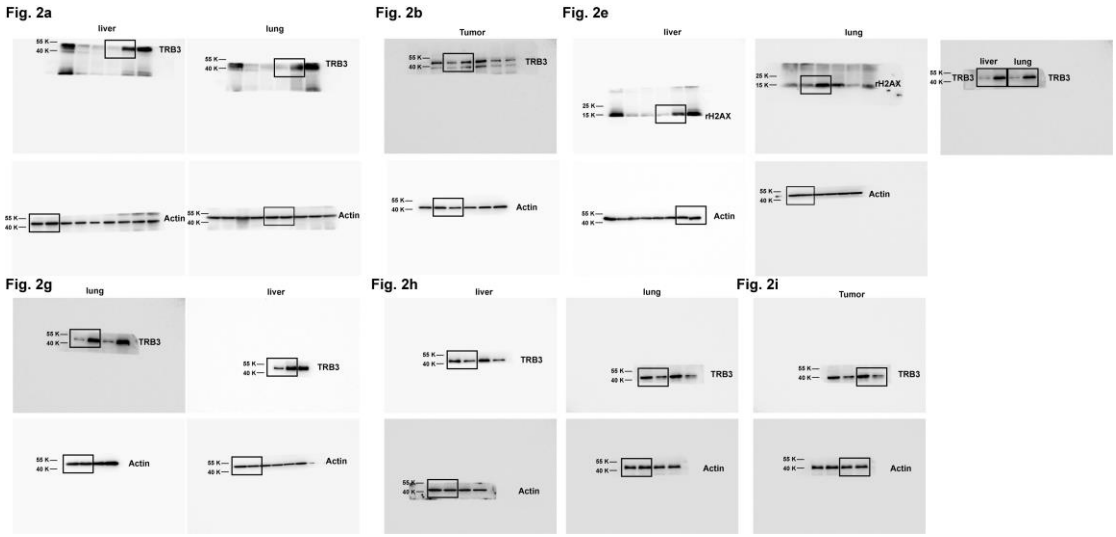

Supplementary Figure 8. Uncropped blots used in Figure 2.

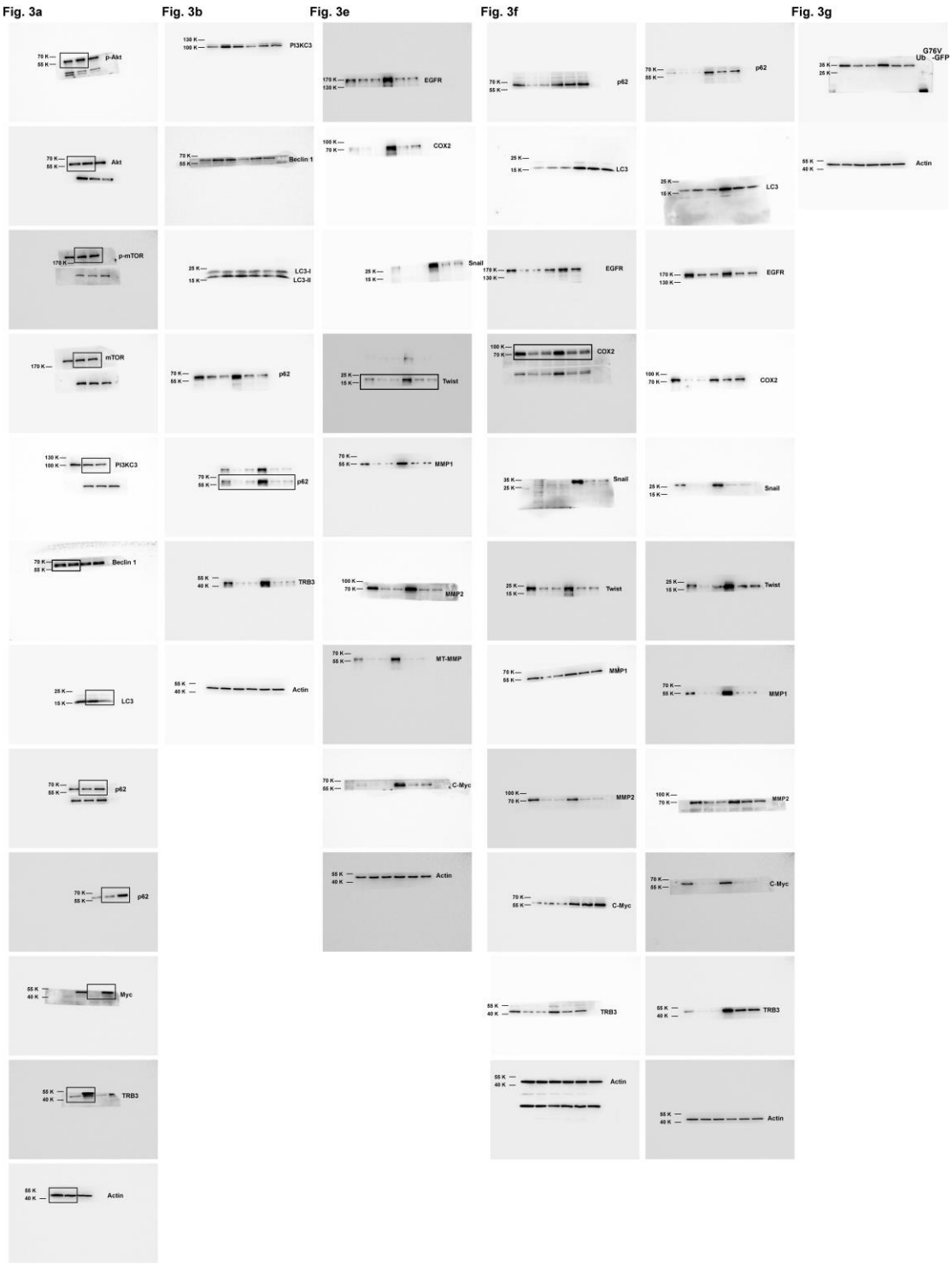

Supplementary Figure 9. Uncropped blots used in Figure 3.

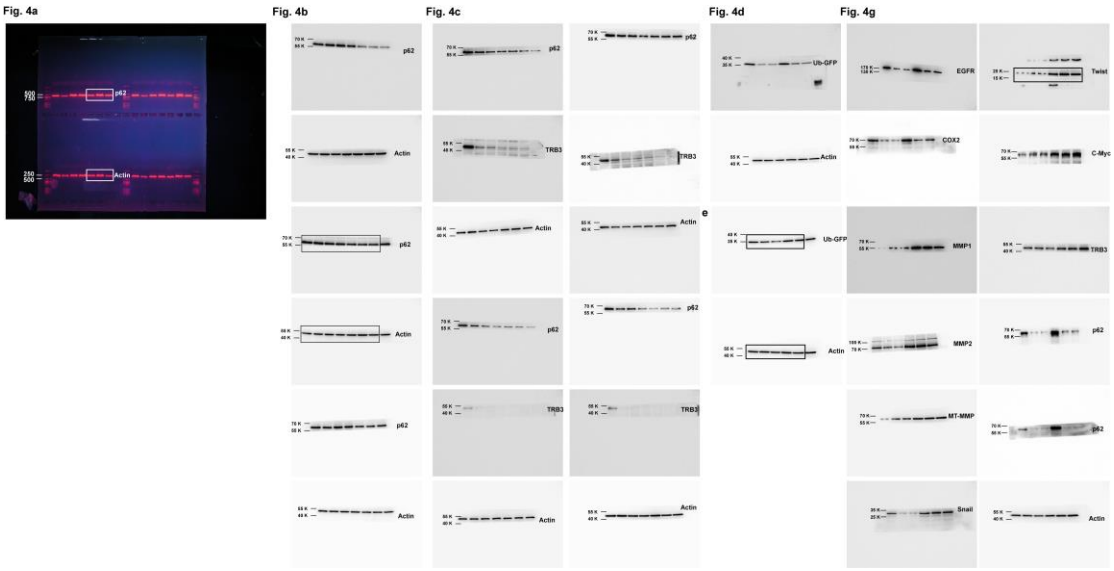

Supplementary Figure 10. Uncropped blots used in Figure 4.

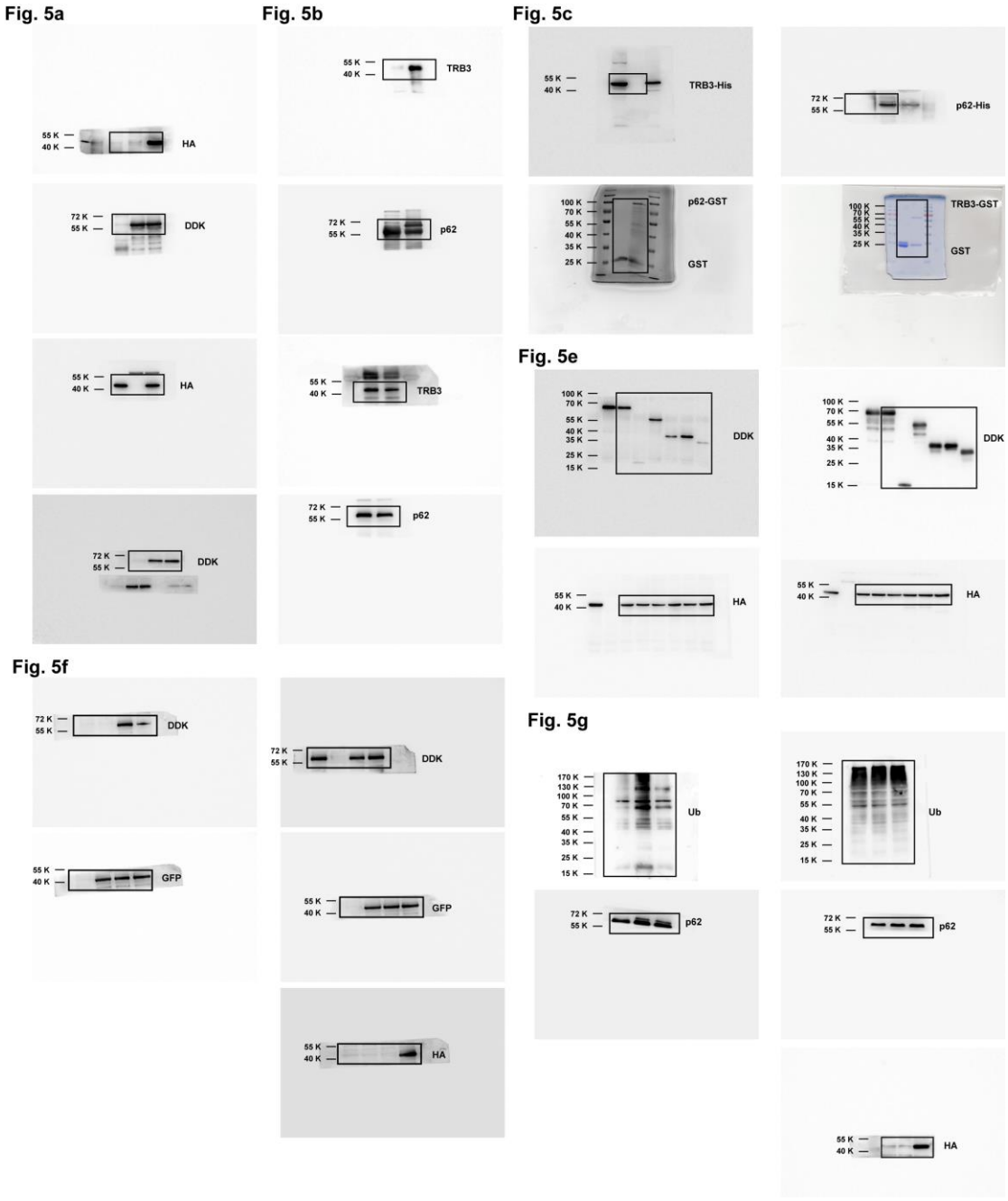

Supplementary Figure 11. Uncropped blots used in Figure 5.

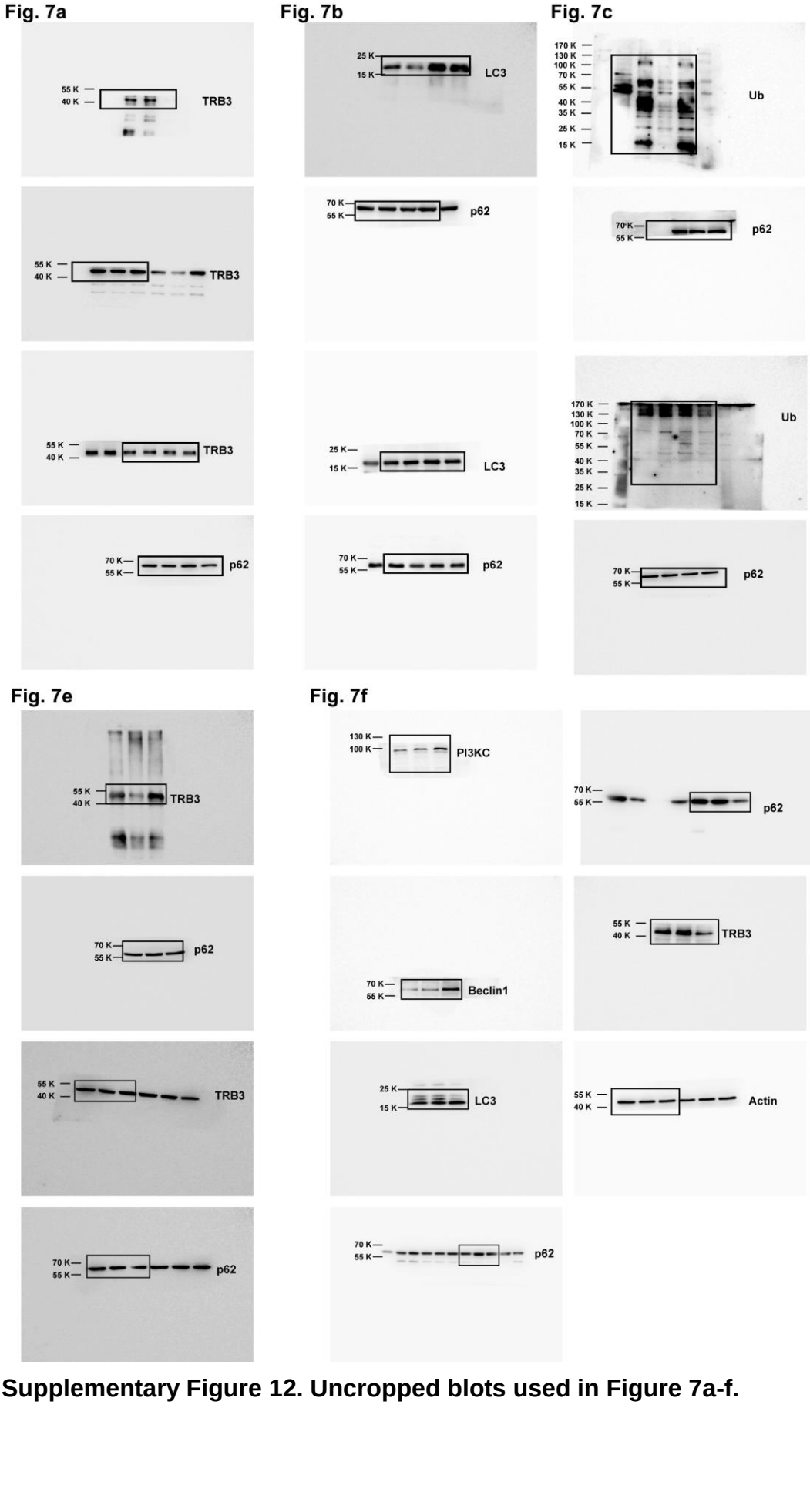

Supplementary Figure 12. Uncropped blots used in Figure 7a-f.

Supplementary Figure 13. Uncropped blots used in Figure 7h-j.

Fig. 8e

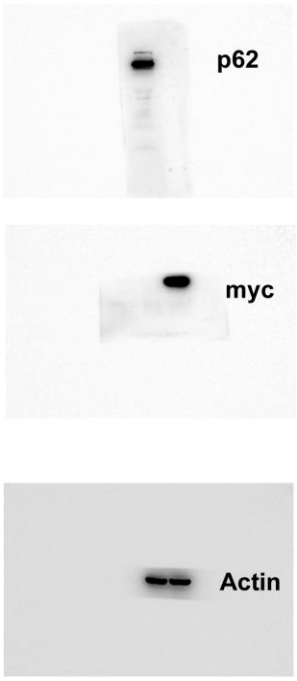

Supplementary Figure 14. Uncropped blots used in Figure 8.

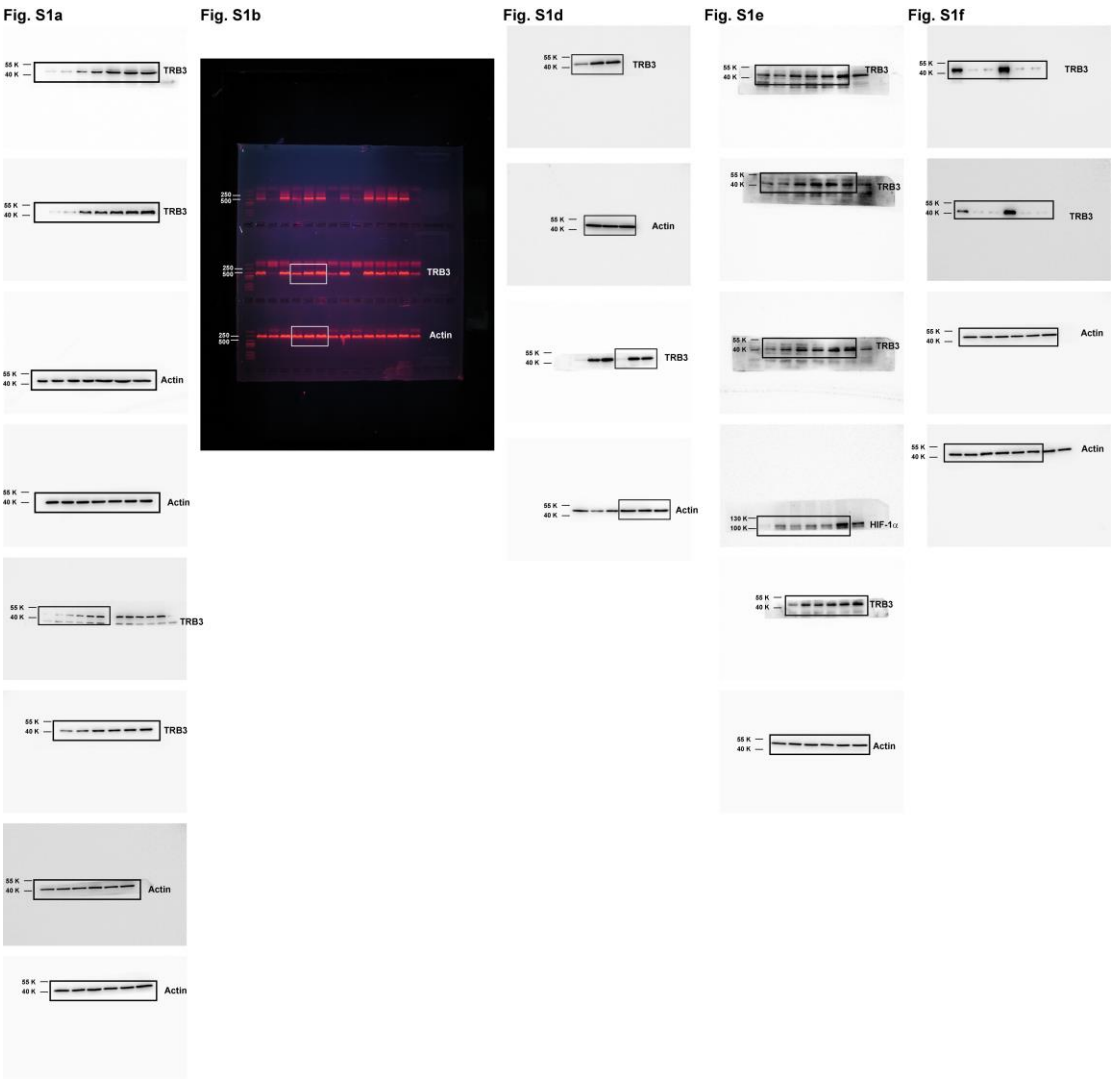

Supplementary Figure 15. Uncropped blots used in Supplementary Figure 1a-f.

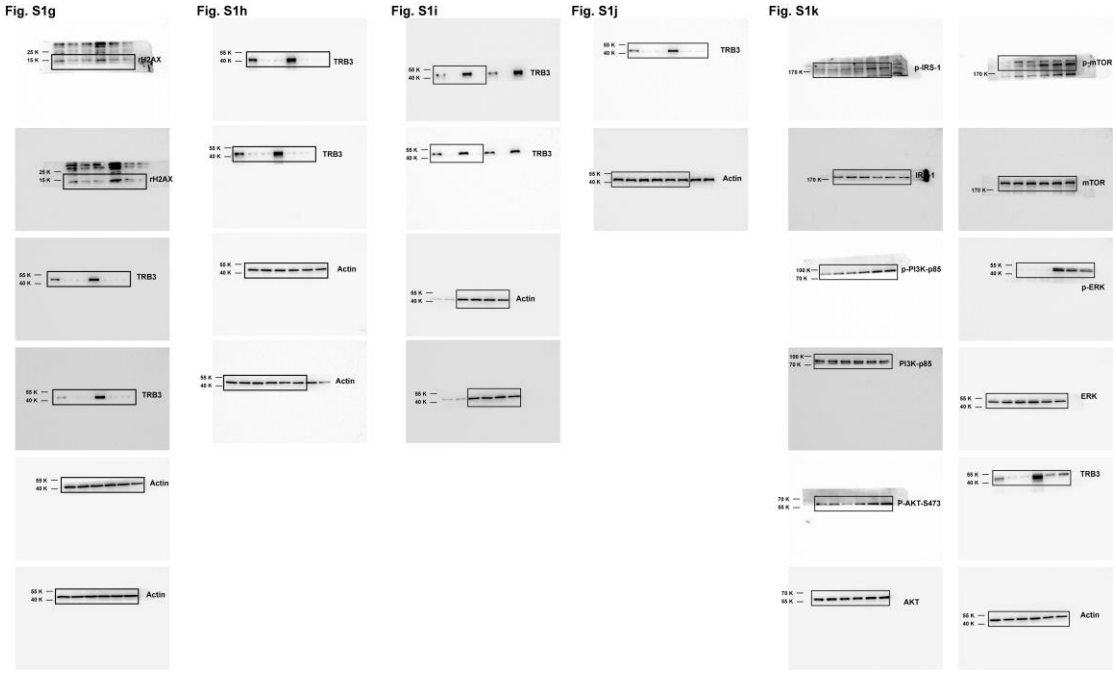

Supplementary Figure 16. Uncropped blots used in Supplementary Figure 1g-k.

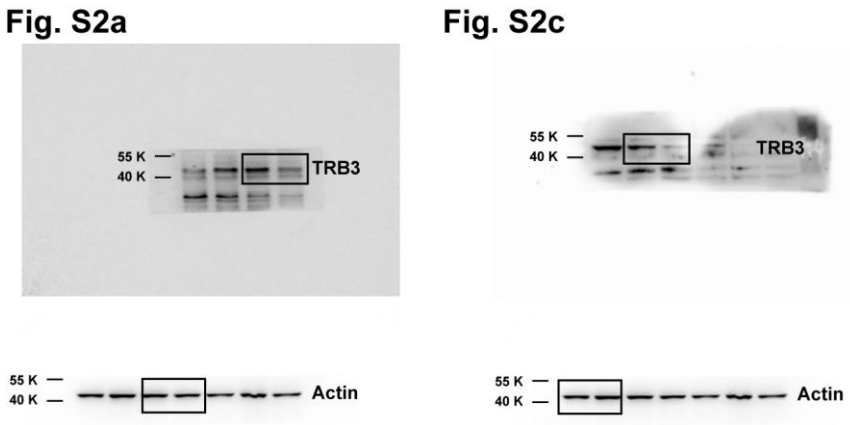

Supplementary Figure 17. Uncropped blots used in Supplementary Figure 2.

Fig. S4b

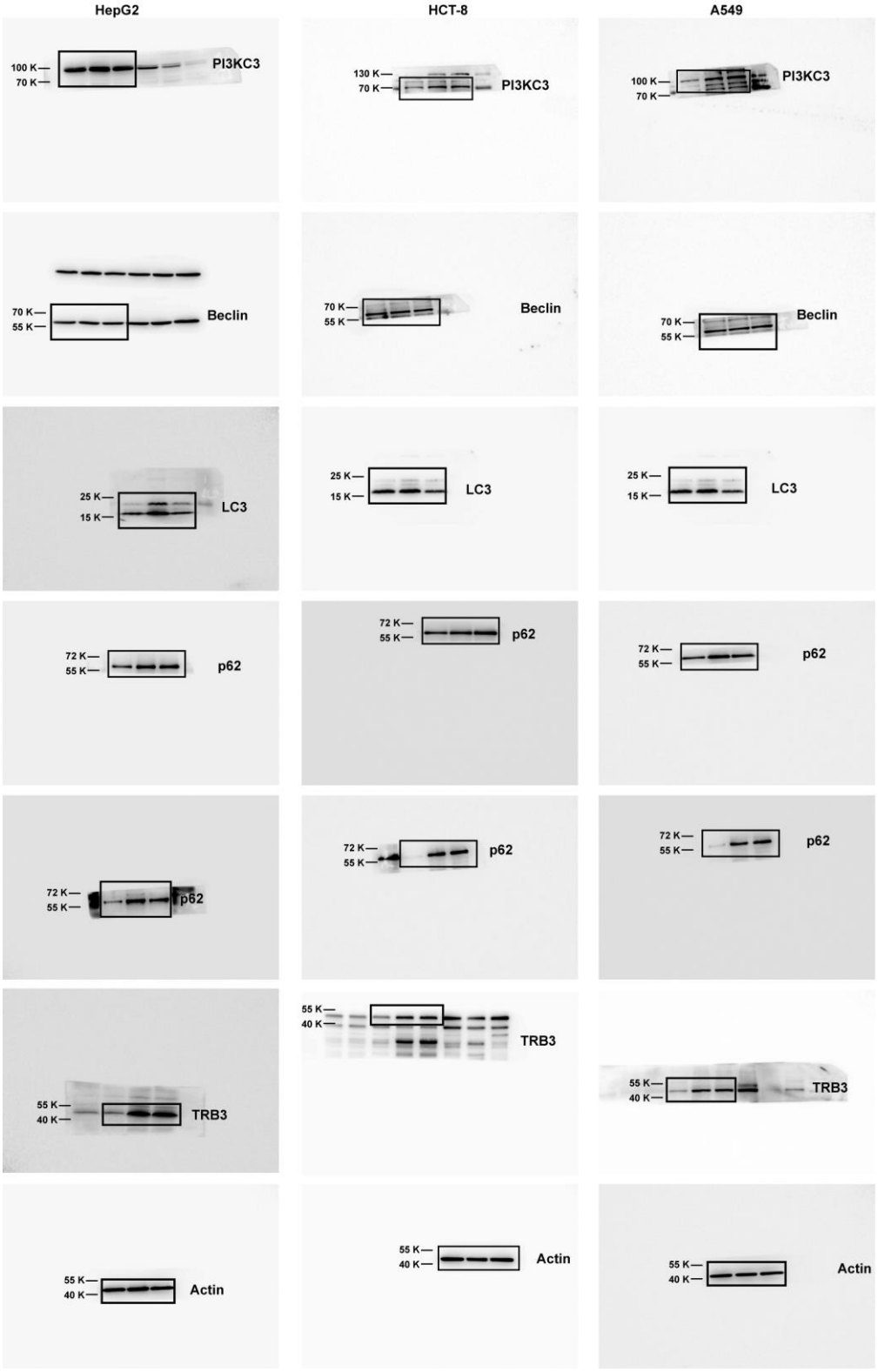

Supplementary Figure 18. Uncropped blots used in Supplementary Figure 4b.

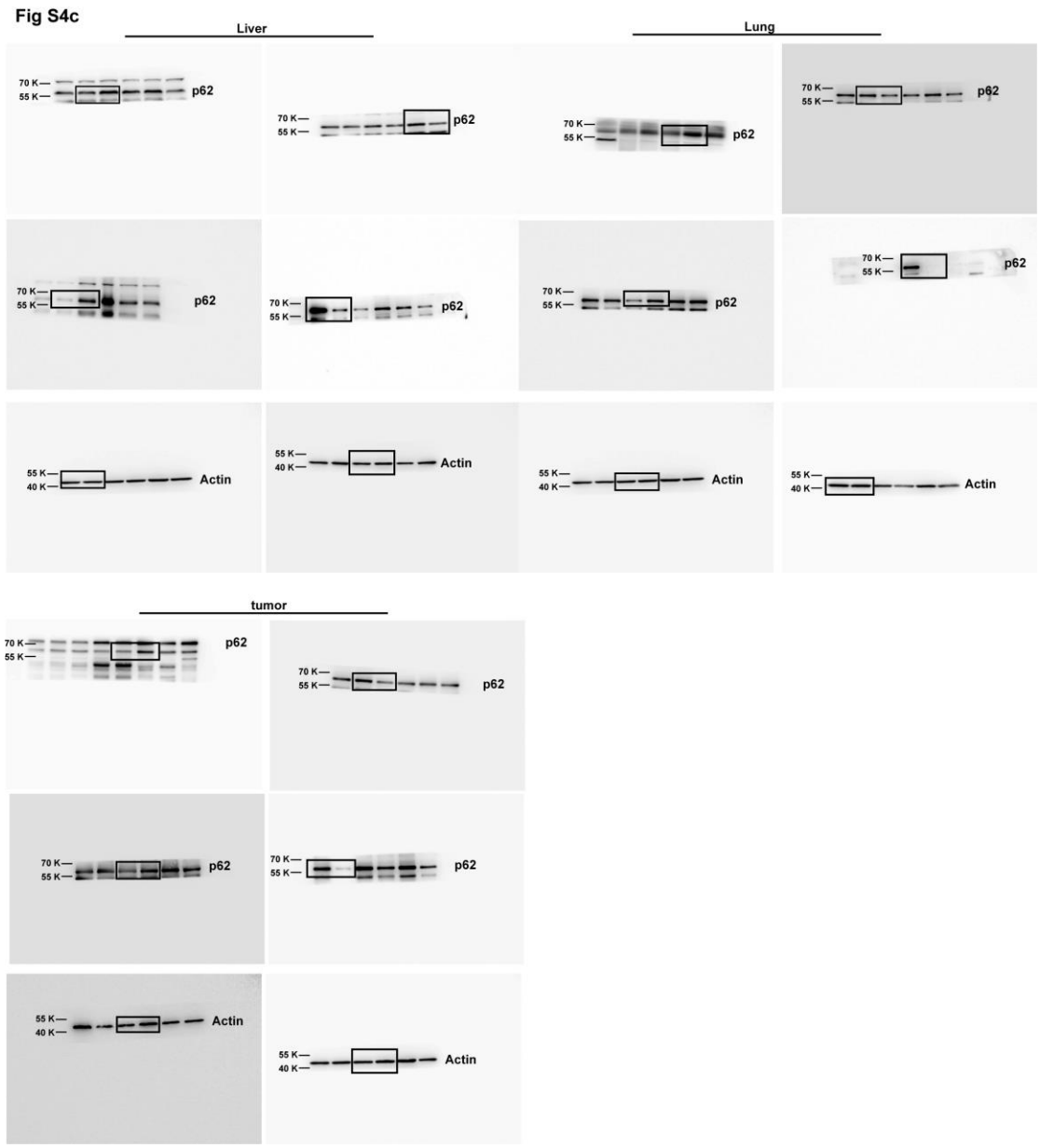

Supplementary Figure 19. Uncropped blots used in Supplementary Figure 4c.

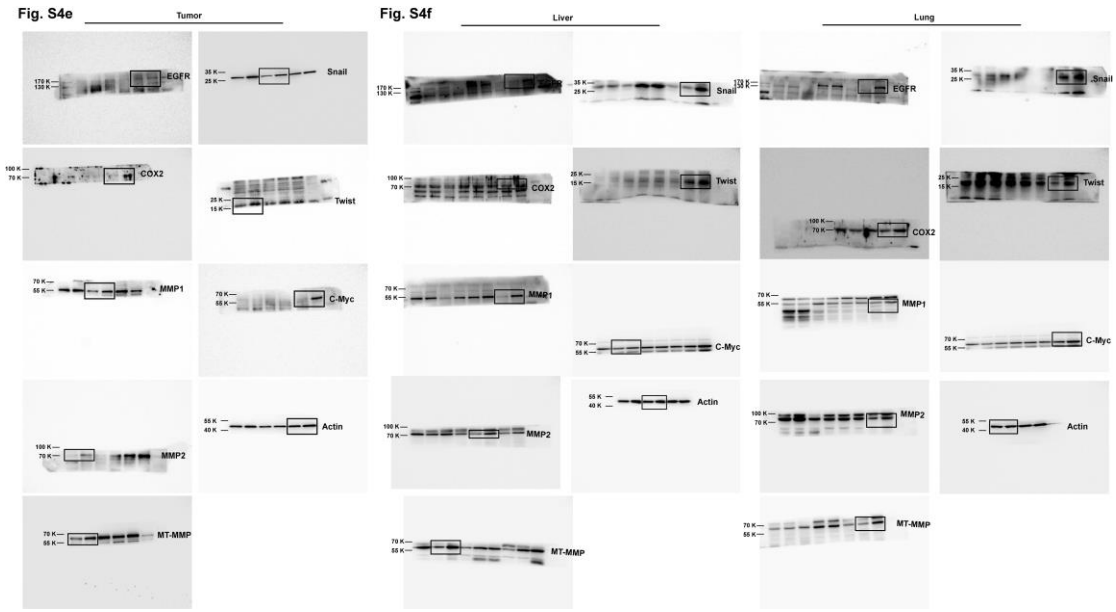

Supplementary Figure 20. Uncropped blots used in Supplementary Figure 4e-f.

Fig. S5a

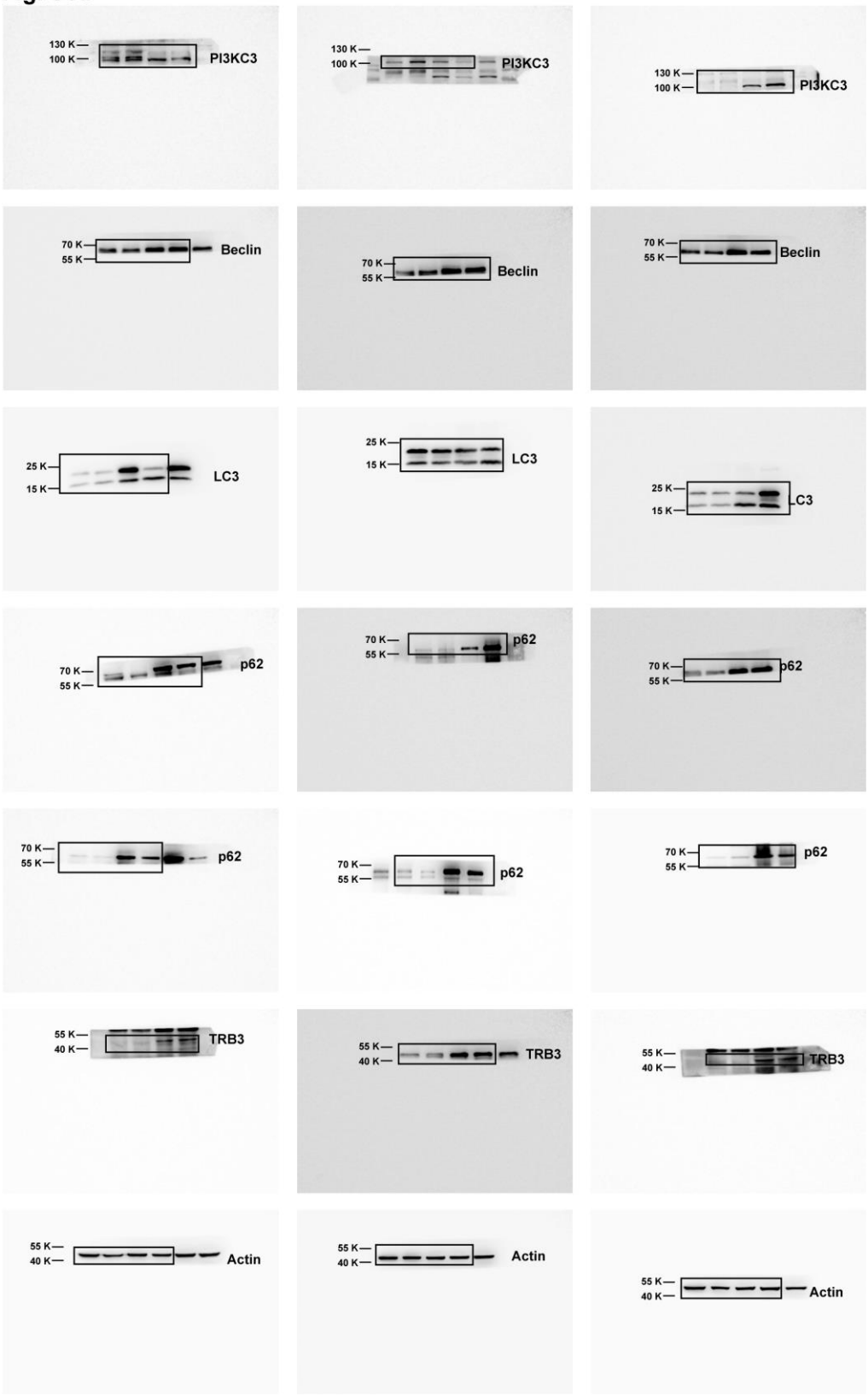

Supplementary Figure 21. Uncropped blots used in Supplementary Figure 5a.

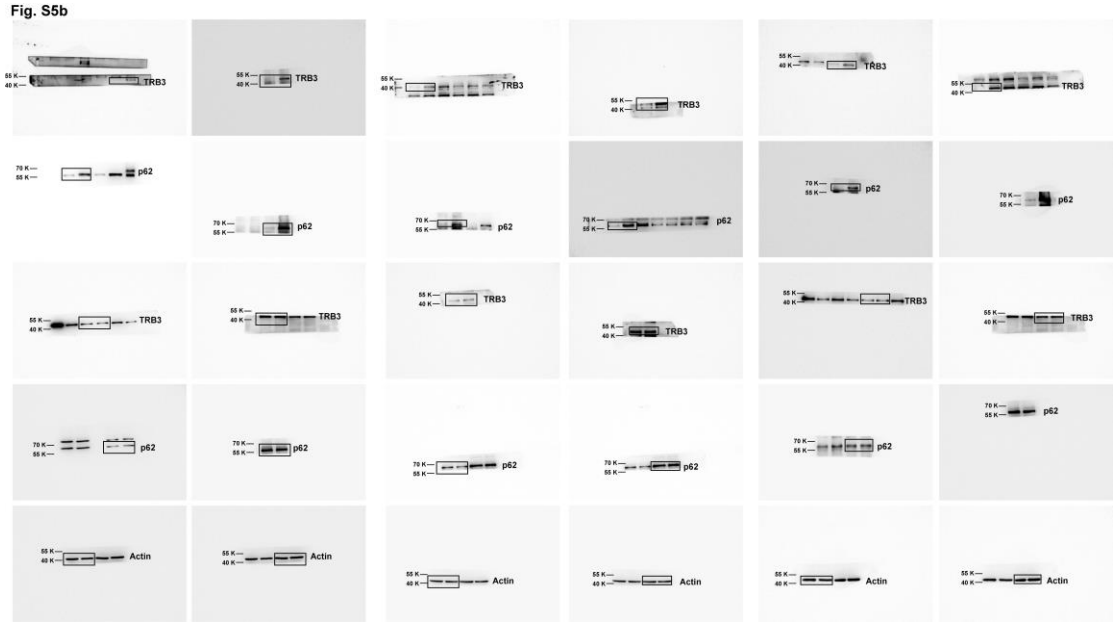

Supplementary Figure 22. Uncropped blots used in Supplementary Figure 5b.

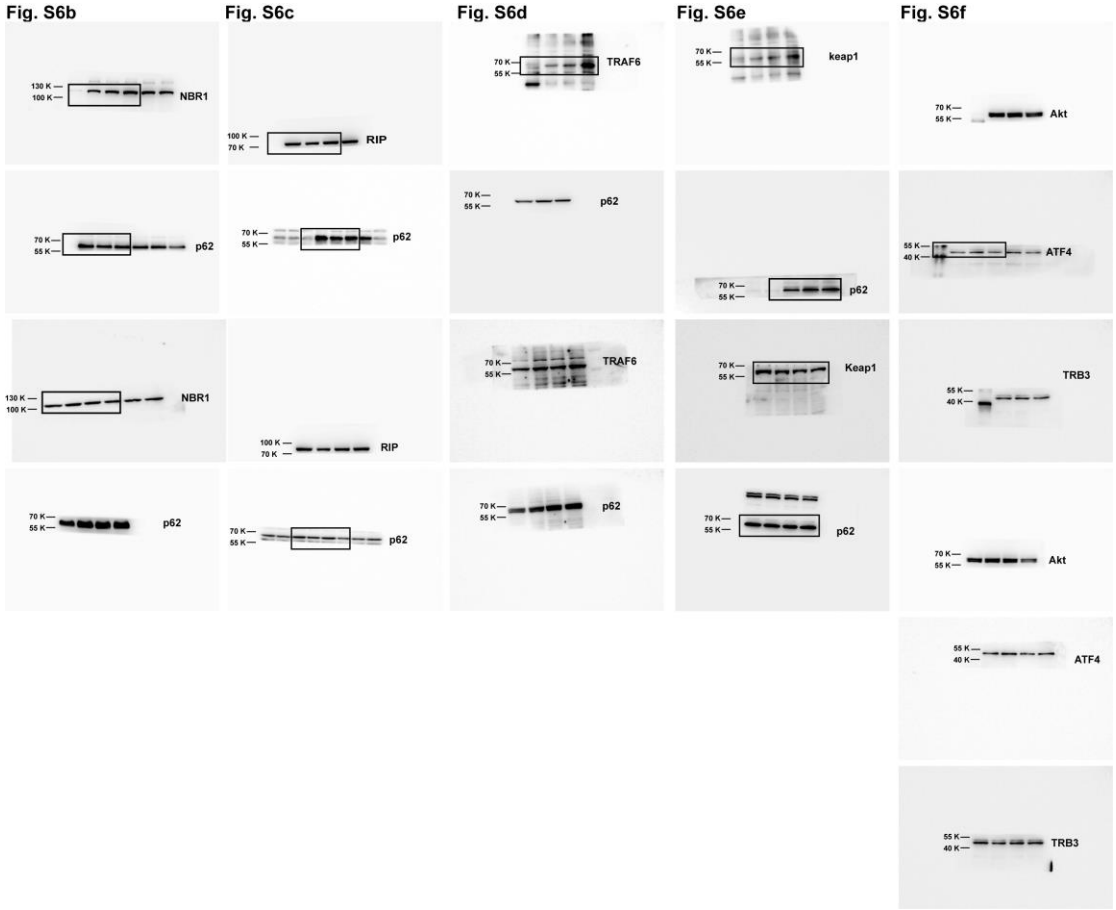

Supplementary Figure 23. Uncropped blots used in Supplementary Figure 6.

Supplementary Table 1. Correlation between TRB3 and pIRS protein expression levels in HCC, colon cancer and lung cancer.

	HCC *n*=71	Colon cancer *n*=69	Lung cancer *n*=65
Protein expression	TRB3 pIRS	TRB3 pIRS	TRB3 pIRS
Pearson r	0.2721	0.283	0.34
P value (two-tailed)	0.0217	0.023	0.004
P value summary	*	*	**

Supplementary Table 2. Multiorgan metastasis of B16-F10 melanoma cells injected intravenously in C57 BL/6 and diabetic KK-Ay mice.

Group	Tissue classes					
	Mesentery	Omentum	Lung	Axillary Lymph Node	Mediastinum	Kidney
C57 BL/6	0.00%	0.00%	50.00%	0.00%	8.33%	0.00%
KK-Ay	45.00%	18.00%	63.00%	36.00%	27.00%	9.09%
KK-Ay/control	0.00%	1.25%	62.50%	25.00%	50.00%	12.50%
KK-Ay/TRB3-KD	0.00%	0.00%	57.10%	0.00%	42.80%	0.00%

*****Each Value shows the percentage of multiorgan metastasis.

Supplementary Table 3. Global protein changes observed in HepG2 cells expressing control-shRNA versus HepG2 cells expressing TRB3-shRNA1.

Supplementary Table 3a

Fold change>1.2 Control-shRNA/TRB3-shRNA1		
Cancer-promoting factor	Cancer-inhibiting factor	Others
EGFR/ErbB1	HADHA	CD30 Ligand/TNFSF8
OSM	IL-9	CD30/TNFRSF8
Glypican 5	CD40 Ligand / TNFSF5 /CD154	IL-4
Frizzled-7	Dkk-3	Siglec-5/CD170
IL-5	Granzyme A	HCR / CRAM-A/B
IL-11	FADD	IL-2 R beta /CD122
FGF-18	HSP60	RELM alpha
Thrombopoietin (TPO)		IL-2 R gamma
MMP-3		CD14
CXCR4 (fusin)		DR6 / TNFRSF21
GM-CSF		IFN-gamma
BMP-5		HCC-4 / CCL16
Frizzled-3		Prolactin
EDG-1		IL-2
Endothelin		IL-3
6Ckine		NT-3
S100A6		FGF-13 1B
VEGF-D		IL-10 R alpha
IL-17		ICAM-5
Insulin		IL-18 R alpha /IL-1 R5
GRO-a		
CCL28 / VIC		
p21		
GRO		
GDF5		
FGF-17		
FGF-5		
PTHLP		
GDF1		
HSP90		
Frizzled-4		
MCP-1		
LRG1		
Frizzled-1		

GCSF		
GDF9		
Cathepsin B		
IL-1 sRI		
E-Selectin		
VEGF R3		
Angiopoietin-like Factor		

Supplementary Table 3b

Fold change < 0.8 Control shRNA / TRB3 shRNA1		
Cancer-promoting factor	Cancer-inhibiting factor	Others
GATA-4	SIGIRR	CD36
TRPM7	AMPKa1	OX40 Ligand / TNFSF4
MMP-20	WIF-1	ApoE3
Neuritin	Cadherin-13	Cytokeratin 8
AFP	ADAMTS-1	IL-1 F8 / FIL1 eta
APN	CRTAM	Calsyntenin-1
ANGPTL3	TNF-beta	11b-HSD1
CRP	Cytokeratin 18	ADAMTS-17
CEA	Afamin	ApoB100
Glut3	SSTR2	Serpin A8
CD44	CNDP1	GPBB
LPS	DEFA1/3	Neurokinin-A
Ras	HOXA10	Alpha 1 AG
FGF-11	FOXN3	2B4
FSH	CBP	SMDF / NRG1Isoform
GLP-1	Calreticulin	BAF57
S100 A8/A9	APC	ESAM
MMP-15	Alpha Lactalbumin	Apelin
ASPH	FABP3	SDF-1 / CXCL12
Factor XIII A	VWF	Thymopoietin
FGFR1 alpha	LECT2	CTACK / CCL27
Tie-1	S100A8	C-peptide
GRP	Presenilin 1	GPR-39
CD59	Clusterin	Amylin
Aldolase A	FRK	VGF
CA 125	KLF4	FoxP3
Apex1	GADD45A	ADAMTS-15
ADAM-9	PTPRD	Procalcitonin
pro-MMP13	IL-29	C5/C5a
SHBG	GDF3	ADAMTS-19
CA 19-9	Chromogranin A	GPI

Mesothelin	E-Cadherin	ADAMTS-18
hCGb	Defensin	cTnT
SPINK1	Thrombospondin-1	Fibrinopeptide A
ABL1	EXTL2	APCS
Aldolase C	Serpin A5	CXCR2 / IL-8 RB
EphA6	EphB3	Growth Hormone (GH)
EphA4	LTF	GMNN
Fyn	MTUS1	Uromodulin
EphA3	Caspase-8	BNP
Thymidine Kinase-1	IL-21	Cytokeratin 19
Kallikrein 10	IL-21 R	C9
CA 15-3	BAI-1	CCK
Desmin	VDUP-1	ApoC1
ALK	Vitamin D Receptor	MSHa
Layilin	Nesfatin	Ceruloplasmin
EphA7	Cystatin A	LYRIC
IL-19	TNK1	ApoA4
ENPP2	Serpin A1	NR3C3
Kallikrein 2		INSRR
ACK1		CD71
Gelsolin		Endorphin Beta
KCC3		BCAM
NAIP		C7
CHI3L1		hCG alpha
Kallikrein 14		MATK
SCG3		IL-12 p70
S-100b		Corticosteroid-binding globulin
NF1		EV15L
Pancreastatin		CK-MB
Calbindin		TRA-1-81
MINA		TSH
Lyn		CART
VE-Cadherin		PSP
HE4		Thyroglobulin
XIAP		TRAIL R1 / DR4 / TNFRSF10A
CA 9		Cystatin C
BMX		GST
PI 3Kinase p85 beta		LTK
FAK		LH
EphB2		Itk
FER		Troponin C
EphA5		C8B
TRA-1-60		FIH
VIP Receptor 2		gamma-Thrombin

uPAR		BD-1
Inhibin A		ProSAAS
EphA8		Creatinine
Endothelin Receptor A		SERPING1
Btk		POMC
Protein p65		Angiopoietin-like 2
Complement factor H		Marapsin
CD46		NPTX1
Calcitonin		NELL2
PSA-total		FGFR1
PAI-1		TXK
GRP75		TPA
Fen 1		Tec
Somatotropin		pro-Glucagon
Hck		Thrombin
Nanog		GFR alpha-4
NET1		SRMS
HSP10		PPARg2
IGF-II R		TRPC6
Trappin-2		NRG3
SART1		
IL-1 R8		
Prohibitin		
Insulin R		
Omentin		
INSL3		
ZAP70		
PSA-Free		
Tyk2		
cIAP-2		
TYRO10		
HSP27		
Ferritin		
COCO		
ROR2		
ACTH		
Kallikrein 11		
Mammaglobin A		
CD74		
MIF		
Erythropoietin R		
IL-13		
ROR1		
TRKB		
RYK		

FGFR2		

(a) Proteins with expression downregulated when silencing TRB3 (Control-shRNA/TRB3-shRNA1>1.2). (b)Proteins with expression upregulated when silencing TRB3 (Control-shRNA/TRB3-shRNA1<0.8).

Supplementary Table 4. Summary of pathological information of human cancer specimens used for immunoblot analysis.

Sample NO.	Age	Gender	Tissue Type	Diagnosis	TNM
1	27	Female	liver	Normal liver tissue	
2	30	Female	liver	Normal liver tissue	
3	35	Male	liver	Normal liver tissue	
4	45	Male	liver	Hepatocellular carcinoma, moderately differentiated	$T_2N_0M_0$
5	51	Male	liver	Hepatocellular carcinoma, poorly differentiated	$T_3N_0M_0$
6	62	Male	liver	Hepatocellular carcinoma, poorly differentiated	
7	59	Male	liver	Hepatocellular carcinoma, moderately differentiated	
8	66	Female	liver	Hepatocellular carcinoma, poorly differentiated	$T_4N_xM_x$
9	24	Male	Colon	Normal colon tissue	
10	25	Male	Colon	Normal colon tissue	
11	40	Female	Colon	Normal colon tissue	
12	75	Male	Colon	Adenocarcinoma, well or moderately differentiated	$T_3N_0M_x$
13	41	Male	Colon	Mucinous adenocarcinoma, poorly differentiated	$T_3N_XM_1$
14	72	Male	Colon	Adenocarcinoma, moderately differentiated	$T_3N_0M_x$
15	61	Female	Colon	Adenocarcinoma, well or moderately differentiated	$T_1N_0M_0$
16	50	Male	Colon	Adenocarcinoma, moderately differentiated	$T_3N_0M_x$
17	28	Male	Lung	Normal lung tissue	
18	28	Male	Lung	Normal lung tissue	
19	25	Female	Lung	Normal lung tissue	
20	60	Female	Lung	Adenosquamous carcinoma	$T_3N_0M_0$
21	52	Female	Lung	Adenosquamous carcinoma	$T_4N_1M_0$
22	70	Male	Lung	Small cell carcinoma and squamous cell carcinoma	$T_4N_1M_X$
23	64	Male	Lung	Adenosquamous carcinoma, moderately differentiated	$T_4N_1M_1$
24	52	Female	Lung	Papillary mucinous adenocarcinoma	$T_4N_1M_X$

Tissues and pathological informations were obtained from Alenabio (Xian, China)

Supplementary Table 5. Multiorgan metastasis of B16-F10 melanoma cells injected intravenously in C57 BL/6 and diabetic KK-Ay mice.

Group	Tissue classes					
	Mesentery	Omentum	Lung	Axillary Lymph Node	Mediastinum	Kidney
C57 BL/6 treated by Pep2-con	0.00%	0.00%	33.3%	0.00%	25.0%	0.00%
C57 BL/6 treated by Pep2-A2	0.00%	0.00%	16.7%	0.00%	25.00%	0.00%
KK-Ay treated by Pep2-con	27.2%	27.2%	54.5%	27.2%	9.09%	9.09%
KK-Ay treated by Pep2-A2	18.1%	9.09%	0.00%	0.00%	0.00%	0.00%

*****Each Value shows the percentage of multiorgan metastasis.

Supplementary Table 6. All primary antibodies against the indicated proteins used in the present study are listed.

Antibody	Provider	Host	Dilution
HA-tag	MBL (561)	Rabbit	1:1000 WB
DDK-tag	MBL (PM020, M185-3)	Mouse/Rabbit	1:1000 WB
Myc-tag	MBL (M047-3)	Mouse	1:1000 WB
GFP-tag	MBL (M048-3)	Mouse	1:1000 WB
LC3	Sigma (L7543)	Mouse	1:100 IF
TRB3	OriGene (TA303408)	Rabbit	1:1000 WB 1:100 IHC
TRB3	Abcam (ab88332)	Mouse	1:100 IF
p62	Sigma (P0067)	Rabbit	1:5000 WB
p62	Abcam (ab56416)	Rabbit	1:500 IF
actin	Cell Signaling Technology (12262)	Mouse	1:1000 WB
beclin 1	Cell Signaling Technology (3495)	Rabbit	1:1000 WB
p-Akt	Cell Signaling Technology (9271)	Rabbit	1:1000 WB
Akt	Cell Signaling Technology (4691)	Rabbit	1:1000 WB
mTOR	Cell Signaling Technology (2972)	Rabbit	1:1000 WB
p-mTOR	Cell Signaling Technology (2971)	Rabbit	1:1000 WB
PI3K p85	Santa Cruz (sc-1637)	Rabbit	1:1000 WB
pPI3K p85	Cell Signaling Technology (4228)	Rabbit	1:1000 WB
ERK	Cell Signaling Technology (4695)	Rabbit	1:1000 WB
pERK	Cell Signaling Technology (4370)	Rabbit	1:1000 WB
γH2AX	Cell Signaling Technology	Rabbit	1:1000 WB

	(2577)		
HIF-1α	Cell Signaling Technology (3716)	Rabbit	1:1000 WB
PI3KC3	Cell Signaling Technology (4263)	Rabbit	1:1000 WB
C-Myc	Cell Signaling Technology (sc-40)	Rabbit	1:1000 WB
COX2	Cell Signaling Technology (12282)	Rabbit	1:1000 WB
EGFR	Cell Signaling Technology (4267)	Rabbit	1:1000 WB
MMP1	Abcam (ab38929)	Rabbit	1:1000 WB
MMP2	Abcam (ab110186)	Rabbit	1:1000 WB
MT-MMP	Abcam (ab53712)	Rabbit	1:1000 WB
Ub	Cell Signaling Technology (3936)	Mouse	1:250 IF
pTyr-100	Cell Signaling Technology (9411)	Mouse	1:1000 WB
Snail	Cell Signaling Technology (3879)	Rabbit	1:1000 WB
Twist	Abcam (ab49254)	Rabbit	1:1000 WB
pIRS-1	Santa Cruz (sc-17196)	goat	1:500 WB 1:100 IHC
IRS-1	Cell Signaling Technology (2382)	Rabbit	1:1000 WB